Letter to the Editor

Length Scale of Disease Spread: Fact or Artifact of Experimental Geometry

Francis J. Ferrandino

Associate scientist, The Connecticut Agricultural Experiment Station, P.O. Box 1106, New Haven 06504.
Accepted for publication 1 May 1996.

To predict the spatial and temporal development of a plant disease epidemic, one needs to quantify the dispersal of inoculum from a focus of disease. But, over what range of distance is this information needed?

To answer this question, one usually measures dispersal experimentally in the field. The results of such an experiment may then be described by an empirical function. However, the general applicability of a fitted dispersal function is intimately tied to the range of distance over which data are taken. Also, the experimental limits of detection can artificially reduce the effective range of distance by censoring data at larger distances from the source of inoculum. An examination of the biases introduced into regression analyses by the geometrical details of the experiment is needed.

Dispersal has most frequently been measured only in close proximity to a source (<5 m), and empirical models fitted to such data are valid only over this range of distance (3,17). The spread of inoculum to larger distances, however, may affect the spatial spread of disease over time (6,10,13,22,33,42). Epidemics of interest often spread to distances in excess of 100 m (20,30). Thus, some assumption about how to extrapolate short-distance measurements to a more general, longer distance distribution of inoculum dispersal is often necessary (14,30,31,32,43,44,45). Gregory (20) and Fitt and McCartney (18) have pointed out the danger of extrapolating a regression equation beyond the fitted distance range. Although the results of any one experiment should not be extrapolated beyond the measured range, it may be possible, by using a wide range of observations covering varying ranges of distance, to obtain general guidelines for extrapolation within reasonable margins of error.

The two most common mathematical models used to fit the observed dispersal of propagules from a focus of disease are the power law model (20):

$$y_P = a'x^{-b} \tag{1A}$$

and the exponential law model (27):

$$y_E = A'e^{-Bx} \tag{1B}$$

in which y is either the deposition density of particles or the resulting lesion density on host plants located at distance x from the focus of the disease. As noted elsewhere (2,18), the major difference between these two expressions is that the exponential law has an implicit length scale, l on the order of B^{-1}, whereas the effective length scale of the power law increases with increasing distance (2). The use of this length scale, l, has been advocated because it is easier to visualize (16,18). However, easy visualization may also lead to misconceptions. In what follows, I will show that values of l reported in the literature are strongly dependent on the geometrical details of the experiment used in their determination. As such, the usefulness of l as a general descriptor of dispersal is questionable.

The above two models are usually first transformed by taking the natural logarithms, yielding:

$$\ln y_P = a - b \cdot \ln x \tag{2A}$$

and

$$\ln y_E = A - B \cdot x \tag{2B}$$

in which

$$a = \ln a' \text{ and } A = \ln A'$$

The model parameters are then fitted by linear regression of $\ln y_P$ on $\ln x$ for the first expression and $\ln y_E$ on x for the second (18). The validity of these regressions hinges on the assumption that the variable y is distributed as a log-normal variate. Such a distribution occurs when a variable can be expressed as the product of many normal variates (36). One can think of these factor variables as a sequence of efficiencies for transport, deposit, wash-off, spore survival, spore germination, and, eventually, infection of the host plant. This is not an unreasonable assumption if counts of lesions or spores remain high enough to keep the stochastic error due to counting at a reasonable level.

The relative suitability of these two empirical fits is usually evaluated by direct comparison of the coefficients of determination, r^2, obtained from the two linear regressions. This comparison can be performed in either the log-transformed space (16,18) or the real space (2). However, any conclusion based on such comparisons without an examination of the errors involved in the determination of the respective r^2 values is suspect.

Thus far, a great deal of effort has been placed on the experimental differentiation of these two empirical equations (2,16,18). However, over a finite length scale these two functions can behave very much alike. One of the implicit problems in any comparison of these two models, based on a measure of relative goodness-of-fit to experimental data, lies in the high degree of correlation that exists between the two alternative spatial variables (x and $\ln x$). This correlation will explicitly depend on the location of the data collection points distributed over the experimentally chosen range of distance. The manner by which this collinearity confounds regression analysis has not been investigated.

The purpose of this letter is threefold: i) to more closely examine the effect of collinearity on the linear regression procedures used to fit disease and dispersal gradients to exponential and power law functions of distance, ii) to examine the implementation of these fitting procedures to experiments reported in the literature, and iii) to attempt to generalize the overall behavior of the length scale parameter fitted to various observations in terms of the pertinent experimental geometry.

Corresponding author: F. J. Ferrandino; E-mail address: fjferr@caes.state.ct.us

Publication no. P-1996-0607-01O

COLLINEARITY AND REGRESSION

To explore the relation between equations 1A and 1B, I will start with a specific example. Assume $A' = 10$ and $B = 1$ m^{-1} in equation 1B so that: $y_E = 10\ e^{-x}$ (Fig. 1, solid line). The power law model (equation 1A) can be fitted to this function if we take the natural logarithm of y_E and then perform a linear regression on ln x. The results of the above regression will depend on the range of distances, x, over which the regression is performed, as well as on the number and spatial distribution of the data points used in the regression. For 10 equally spaced data points between 0.1 and 1 m, the resulting linear regression has a coefficient of determination of 0.906 (Table 1, first column; Fig. 1, dashed line). Repeating this procedure for $B = 2$ m^{-1} ($y_E = 10\ e^{-2x}$) and $B = 3$ m^{-1} ($y_E = 10\ e^{-3x}$) illustrates that the regression scales perfectly with changes in the value of B (Table 1, columns 2 and 3). This scaling is seen graphically in Figure 1 (main panel). If the straight line corresponding to $B = 2$ m^{-1} ($y_E = 10\ e^{-2x}$; Fig. 1, dot-dash line) is scaled so that it overlies the original straight line (Fig. 1, solid line), then the regression lines (Fig. 1, dotted and dashed lines) merge, as well. I now define f to be the ratio of x_{mx} to x_{mn} (i.e., $f = x_{mx}/x_{mn}$), in which x_{mn} and x_{mx} are the minimum and the maximum distance from the source to the data points, respectively. Thus, for a given value of f, the linear regression between y_E and y_P can be characterized by a single curved line-straight line pair plotted between x_{mx} and x_{mn} on the x-axis and between ln[y_E (x_{mx})] and ln[y_E (x_{mn})] on the y-axis. The results of the above scaled regression for values of f = 10, 30, and 100 are shown in Figure 2.

Mathematical details. Given that dispersal data are obtained at the n distances, x_i ($i = 1 \ldots n$), the product-moment correlation between x_i and ln x_i, $R_{x,\ln x}$, can be expressed as:

$$R_{x,\ln x} = \frac{1}{n}\sum_{i=1}^{n}\frac{(x_i - \bar{x})\cdot(\ln x_i - \overline{\ln x})}{\sigma_x \cdot \sigma_{\ln x}} \tag{3}$$

in which the overbar denotes the mean value, and $\sigma_{\ln x}$ and σ_x are the sample standard deviation of ln x_i and x_i, respectively. For any given experiment, the value of the above correlation will depend on the actual geometrical location of the data collection sites. However, the sums in equation 3 can be approximated by integrals if we know the density of data collection points as a function of distance. This procedure results in:

$$R_{x,\ln x} = \frac{\sqrt{3}\cdot\left[f^2 - 1 - 2\cdot f\ \ln(f)\right]}{2\sqrt{(f-1)^2\left\{(f-1)^2 - f\cdot[\ln(f)]^2\right\}}} \tag{4A}$$

if the points are uniformly distributed in x space, and:

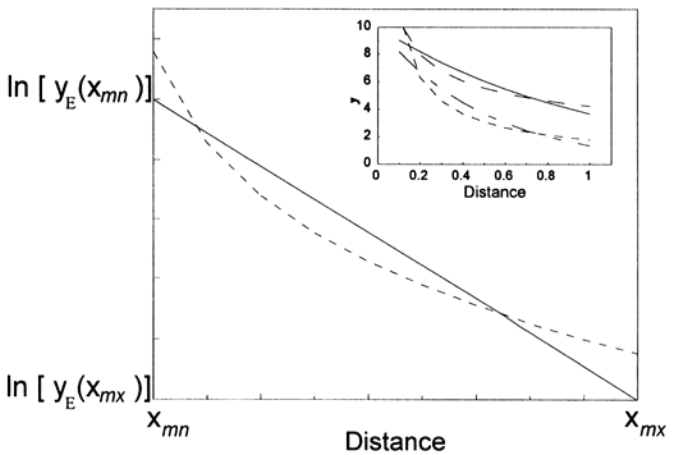

Fig. 1. Plot of deposition density y vs distance x (inset) and ln y vs ln x (main panel) for $y_E = 10e^{-x}$ (solid line), $y_E = 10e^{-2x}$ (dot-dash line), and their respective power law fits (dashed line and dotted line, Table 1 columns 1 and 2).

$$R_{x,\ln x} = \frac{\sqrt{6}\cdot\sqrt{(f^2-1)\cdot\ln(f) - 2\cdot(f-1)^2}}{(f-1)\cdot\ln(f)} \tag{4B}$$

if the points are uniformly distributed in ln x space. Note that $R_{x,\ln x}$ is independent of the fitted parameters (B and b) and only depends on the ratio of x_{mx} to $x_{mn}(f)$. The above approximations for $R_{x,\ln x}$ are presented for the sake of discussion. Their accuracy depends on the true geometric distribution of data collection points. For any particular experiment, the exact value can easily be determined from direct evaluation of the product-moment correlation (equation 3).

Consider now the linear regression of equation 2A on equation 2B:

$$\ln y_P = a - b\ln x = \ln y_E + \varepsilon = A - Bx + \varepsilon \tag{5}$$

In the above regression equation (equation 5), the parameters a and b are assumed given, and the remaining two parameters (A and B) must be chosen so as to minimize the sum of the square errors, $\Sigma\varepsilon_i^2$.

The solution to the above regression yields the following relation between B and b:

$$B = 1/l = bR_{x,\ln x}\,\sigma_{\ln x}/\sigma_x \tag{6}$$

in which $\sigma_{\ln x}$ and σ_x are the sample standard deviations of ln x_i and x_i ($i = 1 \ldots n$), respectively. Combining equation 6 with equation 4A or 4B yields:

$$l = \frac{(x_{mx} - x_{mn})}{3b}\cdot\frac{(f-1)^2}{[f^2 - 1 - 2f\ \ln(f)]} \tag{7A}$$

assuming an homogeneous distribution in the x_i space, and:

$$l = \frac{(x_{mx} - x_{mn})}{b\cdot\ln(f)} \tag{7B}$$

assuming an homogeneous distribution in the ln x_i space. The coefficient of determination in the above regression, $r^2_{x,\ln x}$, is the square of the product-moment correlation (equation 3, Fig. 3).

To discuss the two empirical fits (equations 2A and 2B), it is useful to define the product-moment correlations between ln y_i and x_i, $R_{\ln y,x}$, and between ln y_i and ln x_i, $R_{\ln y,\ln x}$, in analogy with equation 3. The coefficients of determination for the power law model, $r^2_{\ln y,\ln x}$, and the exponential law model, $r^2_{\ln y,x}$, can then be obtained by squaring the appropriate correlations.

STEPWISE REGRESSION

The question at hand is to examine whether or not there is sufficient reason to favor one empirical fit over the other (equations 2A and 2B). Because of the strong collinearity between these two

TABLE 1. Fitted parameters for power law model (equation 2A) obtained by regression to data generated using the exponential law equation (equation 2B). Regressions were performed for 10 equally spaced data points between x_{mn} = 0.1 m and x_{mx} = 1.0 m for various values of parameter B (equation 2B)

y_E	$10\ e^{-x}$	$10\ e^{-2x}$	$10\ e^{-3x}$
Disease level at x = 1 m (a'; eq. 1A)	4.226	1.786	1.325
Standard error of the estimate	0.099	0.197	0.296
Exponent in the power law (b; eq. 1A)	–0.393	–0.786	–1.180
Standard error of b	0.045	0.090	0.135
Coefficient of determination, r^2	0.906	0.906	0.906

functions, it would be advantageous to separate each function into two independent components. One component should represent the commonality in shape between the two functions, and the second component should represent the difference in shape. To this end, I introduce the following ortho-normal pair of predictor variables:

$$Z_{\pm} = \frac{\frac{(\ln x_i - \overline{\ln x_i})}{\sigma_{\ln x}} \pm \frac{(x_i - \overline{x_i})}{\sigma_x}}{2 \cdot (1 \pm R_{x,\ln x})} \quad (8)$$

Note that Z_+ is a functional average of the x and $\ln x$ functions and that Z_- is a measure of the difference between these two functions. One now performs a stepwise linear regression using the model:

$$\ln y = C_0 + C_+ Z_+ + C_- Z_- \quad (9)$$

in which the C parameters are fitted by regression.

One can conceptualize the nature of all of the above regressions (equations 2A, 2B, 5, and 9) in terms of a three-dimensional space defined by Z_+, Z_-, and an error axis, ε, that is normal to the Z_+-Z_- plane (Fig. 4). The data vector, ln y, will lie above this plane with a vertical component, s, corresponding to the error in the Z_+, Z_- regression, in which s^2 is equal to the residual sum of squares from the above model (equation 9, Fig. 4). The power law, P, and exponential law, E, models can be conceived of as two vectors lying in the Z_+-Z_- plane (Fig. 4). The cosine of the angle between any two vectors is equal to the product-moment correlation, so that $R_{x,\ln x} = \cos \alpha$, $R_{\ln y,\ln x} = \cos \beta$, and $R_{\ln y,x} = \cos \gamma$ (Fig. 4).

If the data vector lies directly above the Z_+-axis in Figure 4, then $C_- = 0$ ($\beta = \gamma$), and the data are described equally well by the power law or exponential model. Thus, the statement that the exponential law and the power law fits can be statistically differentiated is equivalent to rejecting the null hypothesis H_0:$C_- = 0$. This can be accomplished by comparing the value of $r^2_{\ln y,Z-}$, the extra sum of the squares because of the inclusion of Z_- in equation 9, with s^2 by an $F(1, n-3)$ test (11,40), in which $n-3$ is the number of degrees of freedom on which the estimate of error, s^2, is based (11). Defining the projection of the data vector (ln y; Fig. 4) on the Z_+ and Z_- unit vectors as R_+ and R_-, respectively, this comparison can be obtained from an extension of the Pythagorean theorem: $(\ln y)^{-2} = s^2 + R_+^2 + R_-^2$. The value of this F is given by:

$$F = \frac{(n-3) \cdot r^2_{\ln y,Z_-}}{(1 - r^2_{\ln y,Z_+} - r^2_{\ln y,Z_-})} \quad (10)$$

Using the definitions of Z_+ (equation 8) and the known correlations between x, ln x, and ln y, equation 10 becomes:

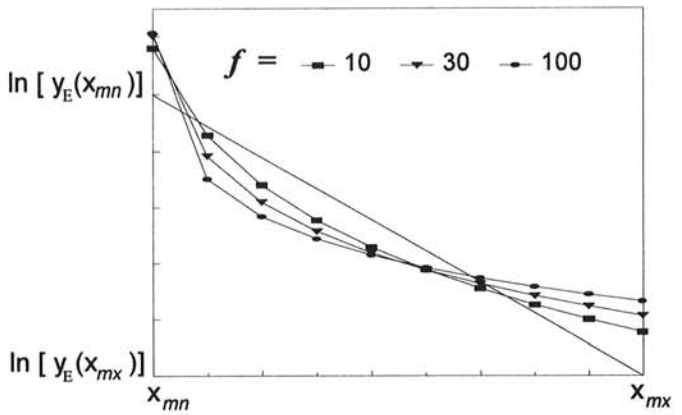

Fig. 2. Comparison of y_E (solid line) and fitted value of y_P for various values of the ratio of farthest distance to nearest distance, f.

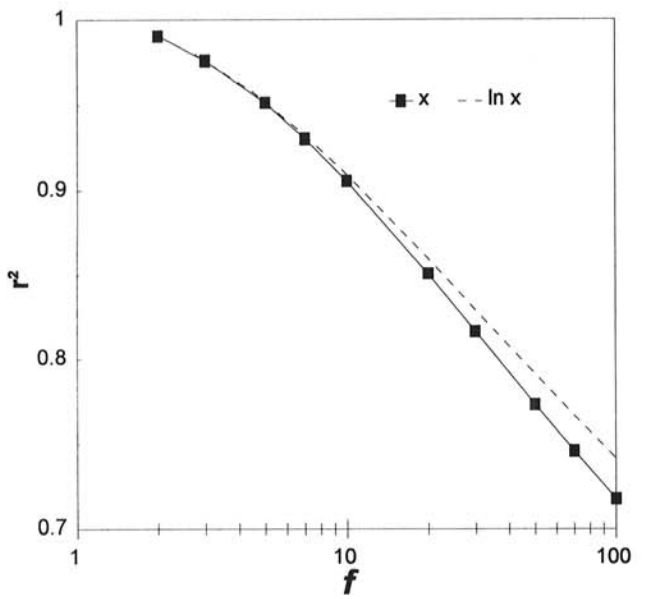

Fig. 3. Plot of the coefficient of determination for the ln y_E (equation 2A) vs ln y_P (equation 2B) regression vs ln f for equally spaced points in x space (solid line, the square of equation 4A), equally spaced points in ln x space (dotted line, the square of equation 4B), and the regressions shown in Figure 2 (squares).

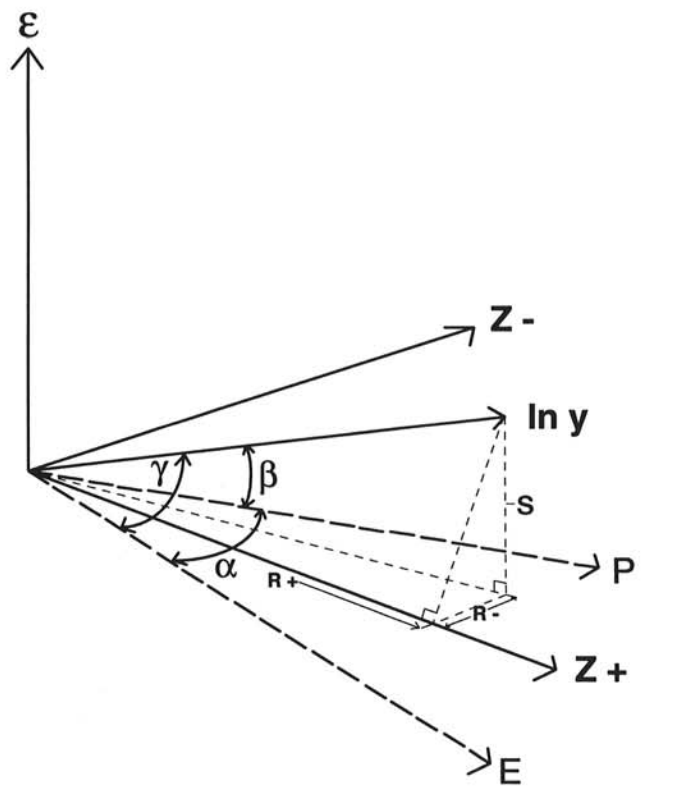

Fig. 4. Geometric representation of regressions discussed in text. The vector labeled ln y represents the log transform of the observed data. P and E are unit vectors representing the power law (ln x) and exponential law (x) independent variables. $Z_\pm$ are the transformed regression variables defined in equation 8. The ε-axis corresponds to the error, s, not fit by the regression in equation 9.

$$F = \frac{(n-3)\cdot(1+R_{x,\ln x})\cdot(R_{\ln y,\ln x}-R_{\ln y,x})}{2\cdot(1-r^2_{x,\ln x}-r^2_{\ln y,x}-r^2_{\ln y,\ln x}+2R_{x,\ln x}R_{\ln y,x}R_{\ln y,\ln x}} \quad (11)$$

To apply this test, the various correlations appearing in equation 11 are calculated and the value of F obtained is compared with tabulated values (40). If the F value is significant, then one is justified in rejecting the null hypothesis (H_0:$C_- = 0$), and one of the two models (equations 2A and 2B) provides a significantly superior fit to the data.

GEOMETRICAL MODEL

I propose a simple geometrical model to predict the observed length scale obtained from a regression of ln y on x. Deposition about a point source is assumed to be described by an inverse square law of distance, so that $b = 2$ in equations 7A and 7B. This "Radiative model" (5) assumes that spores travel analogously to radiation in straight lines away from their point of origin and, thus, spread out in both the vertical and horizontal directions. If the source of inoculum is a line with a length greater than x_{mx}, then I will assume $b = 1$ in equations 7A and 7B (20), since the horizontal spread of spores will have no effect on spore deposit. In addition, to account for the effect of source size on the initial spatial variance of the spore cloud for an extended source, I make an ad hoc assumption that all distances be increased by an amount r_s defined below. This is analogous to the empirical modification of the power law suggested by Mundt and Leonard (34). Using equation 7B and the above assumptions, I propose the following predictor equations for length scale, l:

$$l_P = \frac{(x_{mx}-x_{mn})}{2\ \ln[(x_{mx}+r_s)/(x_{mn}+r_s)]} \quad (12A)$$

$$l_L = \frac{(x_{mx}-x_{mn})}{\ln(x_{mx}+r_s)/(x_{mn}+r_s)]} \quad (12B)$$

in which r_s is the half-width of the source, which, for an extended area source (a generalized point source equation 12A, subscript P) of length L and width W, is defined by $r_s = (LW)^{0.5}/2$, and for a line source of length L and finite width W (generalized line source equation 12B, subscript L), is defined by $r_s = W/2$. The derivation that led to equations 12A and 12B could also be performed using equation 7A for spatially homogeneous data points in the real space. However, over the range of values reported for x_{mn} and x_{mx} in the literature, this algebraically more complicated result is well approximated by equations 12A and 12B. Note that equations 12A and 12B depend only on the experimental geometry, and all of the necessary parameters (x_{mx}, x_{mn}, and r_s) are known before data are even collected.

RESULTS AND DISCUSSION

Linear regression analyses (equation 9) were applied to 105 profiles obtained from the literature (Table 2). The regression results revealed that 51 of the data sets were fitted better by the exponential law model and 54 were fitted better by the power law model, based on a simple comparison of the coefficients of determination (r^2). However, further analyses based on the F test criterion (equations 12A and 12B) revealed that only six of the 51 cases favoring the exponential law model and 15 of the 54 cases favoring the power law model were significant ($P < 0.05$, Table 2). In general, experiments with a point source of inoculum tended to favor an exponential law fit, and experiments with line sources of inoculum favored the power law.

In making the above 105 comparisons, one expects some spurious false positives (Type I error). Remembering that both tails of the distribution are flagged at the 5% level, pure random chance would predict nine cases that mistakenly favor the exponential law and nine cases that mistakenly favor the power law (40). Overall, the above collection of comparisons showed little preference for either empirical model, as 80% of the profiles were described equally well by the power law (equation 1A) or the exponential law (equation 1B) equation. This is in basic agreement with the results of Fitt et al. (16) and bold testimony to the fact that these two functions can behave very similarly.

Taken singly, the results of these experiments can be well described by the exponential law. However, the values of l predicted

TABLE 2. Literature references and geometrical details for the 105 dispersal profiles used in the text

Authors	Reference	x_{mn} (m)	x_{mx} (m)	r_s (m)	f	l (m)
Point sources						
Alderman et al.	1	0.15	1.4	0.3	6–9	0.2–0.4
Brennan et al.	8	0.1	0.8	0.05	4–8	0.04–0.1
Cammack	9	5	40	0.1	8	7–9
Fatemi and Fitt	12	0.1	0.9	0.05	5–9	0.1–0.2
Ferrandino and Aylor	14	1	16	0.5	5–8	0.8–3.3
Fried et al.	19	0.12	8	0.1	67	1.2–1.5
Jeger et al.	23	0.4	2	0.1	5	0.3
Jones and Newhall	25	25	302	20	12	71–77
Minogue and Fry	32	0.5	9	0.5	5–10	0.4–1.4
Newhall	35	37	1,000	12	28	120
Sreeramulu and Ramalingam	41	2.5	45	0.01	3–12	5–16
Extended area sources						
Heald et al.	21	4.6	127	64–120	15–26	60–170
Johnson and Dickson	24	12	130	11	11	18
McCartney et al.	29	0.5	19	23	37	11–14
Raynor et al.	37	1	60	9	60	13–21
Roelfs	38	2	73	32	37	24–30
Schneiderhahn	39	59	4,830	400–1,000	2–20	2,000–2,800
Line sources						
Aylor	2	0.1	3.7	0.4–0.7	30–37	0.7–1.7
Aylor and Ferrandino	4	1.6	29	0.2	7–18	2–7
Bertrand and English	7	1.2	38	0.1	8–32	1.4–6
Ferrandino and Elmer	15	0.5	32	0.5	8–32	1.4–8
Gregory	20	1	30	0.7	20–30	4–8
Keitt et al.	26	46	137	12	3	71
McCartney and Bainbridge[a]	28	0.15	1.5	0.05	10	0.4–0.7

[a] In this study, deposition was totaled within annular rings. This is equivalent to a line source (20).

by regression analysis (Table 2) range over four orders of magnitude. Thus, it is impossible to fit all the profiles with one length scale. The generality of the power law model fares much better. To test the model embodied in equations 12A and 12B, the observed length scales, l, are plotted versus the appropriate predictions (l_P or l_L depending on the source geometry) in a log-log plot (Fig. 5). The model predictions are based on an assumed inverse square law of distance and depend only on the geometrical details of the experiment (equations 12A and 12B). The standard error of the observed length scales about the 1:1 line in Figure 5 is 0.32, which corresponds to relative standard error of about 33%. This is quite remarkable considering the great variation in wind speed, particle size, canopy height, and vegetation density represented in the experimental sample. Given the complexity of the release, transport, and deposit of spores, it is interesting and encouraging that so much of the variation in the observed behavior can be described in terms of the experimental geometry.

The strong dependence the length scale obtained from a regressive fit to the exponential distance law (equation 2A) on the geometric vagaries of a particular experiment suggests that l may not be a suitable parameter to describe spore dispersal in an epidemiological model. Furthermore, one must be wary in interpreting any derived dependence of fitted length scale upon meteorological or biological variables without first examining the geometry of the experiment. As an example, Bertrand and English (7) found that wind speed had a strong effect on the fitted dispersive length scale for conidia of *Valsa leucostoma* released in the rain. However, in their experiments, increased wind speed also increased the overall magnitude of spore dispersal that allowed measurements out to larger distances. In general, any variable that affects the amount of spores released may change the distance range of measurements and, therefore, geometrically bias the fitted value of the length scale.

CONCLUSIONS

A geometrical dispersal model has been presented that explains most of the observed variation in fitted dispersive length scale over four orders of magnitude (0.13 m to 2800 m). The success of this model (equations 12A and B, Fig. 5) provides a guideline for extrapolation of short-ranged dispersal measurements to larger distances. That is not to say that the inverse square law is the correct mechanistic model for dispersal. Rather, these results suggest that the underlying geometrical principles embodied in equations 12A and 12B are common to all the above dispersal experiments.

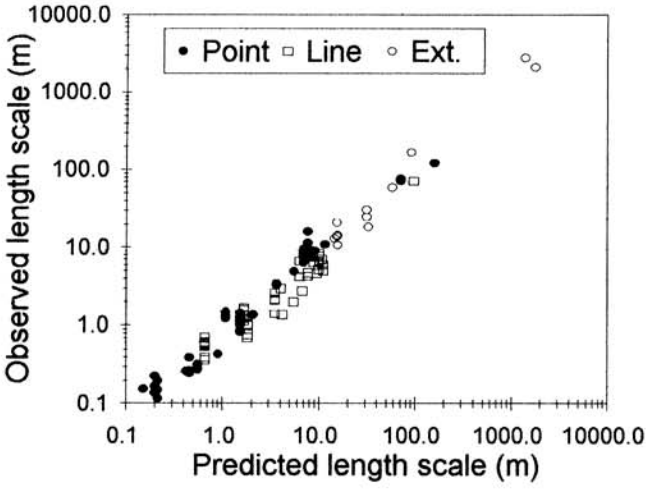

Fig. 5. Plot of ln l from the observed dispersal profiles reported in Table 2 vs the log of the predictive equation (equations 12A and 12B). Point sources (filled circles), extended point sources (open circles), and line sources (open squares).

The results of any one experiment can always be better fit by an empirical equation valid only within the distance range of measurement. However, the above analyses suggest that the assumption of a dispersive length scale determined by geometrical extent remains robust over a large range of distances and meteorological conditions. Thus, the distance range over which dispersal must be quantified will be directly determined by the size of the field under study.

LITERATURE CITED

1. Alderman, S. C., Nutter, F. W., Jr., and Labrinos, J. L. 1989. Spatial and temporal analysis of spread of late leaf spot of peanut. Phytopathology 79:837-844.
2. Aylor, D. E. 1987. Deposition gradients of urediniospores of *Puccinia recondita* near a source. Phytopathology 77:1442-1448.
3. Aylor, D. E. 1989. Aerial spore dispersal close to a focus of disease. Agric. For. Meteorol. 47:109-122.
4. Aylor, D. E., and Ferrandino, F. J. 1989. Temporal and spatial development of bean rust epidemics initiated from an inoculated line source. Phytopathology 79:146-151.
5. Aylor, D. E., and Ferrandino, F. J. 1990. Initial spread of bean rust close to an inoculated bean leaf. Phytopathology 80:1469-1476.
6. Berger, R. D., and Luke, H. H. 1979. Spatial and temporal spread of oat crown rust. Phytopathology 69:1199-1201.
7. Bertrand, P. F., and English, H. 1976. Release and dispersal of conidia and ascospores of *Valsa leucostoma.* Phytopathology 66:987-991.
8. Brennan, R. M., Fitt, B. D. L., Taylor, G. S., and Colhoun, J. 1985. Dispersal of *Septoria nodorum* pycnidiospores by simulated raindrops in still air. Phytopathol. Z. 112:281-290.
9. Cammack, R. H. 1958. Factors affecting infection gradients from a point source of *Puccinia polysora* in a plot of *Zea mays.* Ann. Appl. Biol. 46:186-197.
10. Diekmann, O. 1978. Thresholds and traveling waves for the geographical spread of infection. J. Math. Biol. 6:109-130.
11. Draper, N. R., and Smith, H. 1981. The "extra sum of squares" principle. Pages 97-102 in: Applied Regression Analysis, 2nd ed. John Wiley & Sons, Inc., New York.
12. Fatemi, F., and Fitt, B. D. L. 1983. Dispersal of *Pseudocercosporella herpotrichoides* and *Pyrenopeziza brassicae* spores in splash droplets. Plant Pathol. 32:401-404.
13. Ferrandino, F. J. 1993. Dispersive epidemic waves: I. Focus expansion within a linear planting. Phytopathology 83:795-802.
14. Ferrandino, F. J., and Aylor, D. E. 1987. Relative abundance and deposition gradients of clusters of urediniospores of *Uromyces phaseoli.* Phytopathology 77:107-111.
15. Ferrandino, F. J., and Elmer, W. H. Septoria leaf spot lesion density on trap plants exposed at varying distances from infected tomatoes. Plant Dis. In press.
16. Fitt, B. D. L., Gregory, P. H., Todd, A. D., and McCartney, H. A. 1987. Spore dispersal and plant disease gradients; a comparison between two empirical models. J. Phytopathol. 118:227-242.
17. Fitt, B. D. L., and Lysandrou, M. 1984. Studies on mechanisms of splash dispersal of spores using *Pseudocercosporella herpotrichoides* spores. Phytopathol. Z. 111:323-331.
18. Fitt, B. D. L., and McCartney, H. A. 1986. Spore dispersal in relation to epidemic models. Pages 311-345 in: Plant Disease Epidemiology. K. J. Leonard and W. E. Fry, eds. MacMillan Publishing Co., Inc., New York.
19. Fried, P. M., MacKenzie, D. R., and Nelson, R. R. 1979. Dispersal gradients from a point source of *Erysiphe graminis* f. sp. *tritici*, on Chancellor winter wheat and four multilines. Phytopathol. Z. 95:140-150.
20. Gregory, P. H. 1968. Interpreting plant disease dispersal gradients. Annu. Rev. Phytopathol. 6:189-212.
21. Heald, F. D., Gardner, M. W., and Studhalter, R. A. 1915. Air and wind dissemination of ascospores of the chestnut-blight fungus. J. Agric. Res. 3:493-526.
22. Jeger, M. J. 1983. Analyzing epidemics in space and time. Plant Pathol. 32:5-11.
23. Jeger, M. J., Jones, D. G., and Griffiths, E. 1983. Disease spread of non-specialized fungal pathogens from inoculated point sources in intra-specific stands of cereal cultivars. Ann. Appl. Biol. 102:237-244.
24. Johnson, A. G., and Dickson, J. G. 1919. Stem rust of grains and the barberry in Wisconsin. Wis. Agric. Exp. Stn. Bull. 304:1-16.
25. Jones, M. D., and Newall, L. C. 1946. Pollination cycles and pollen dispersal in relation to grass improvement. Nebr. Agric. Exp. Stn. Bull. 148:1-43.
26. Keitt, G. W., Clayton, C. N., and Langford, M. H. 1941. Experiments with eradicant fungicides for combating apple scab. Phytopathology 31:296-322.

27. Kiyosawa, S., and Shiyomi, M. 1972. A theoretical evaluation of the effect of mixing resistant variety with susceptible variety for controlling plant disease. Ann. Phytopathol. Soc. Jpn. 38:41-51.
28. McCartney, H. A., and Bainbridge, A. 1984. Deposition gradients near to a point source in a barley crop. Phytopathol. Z. 109:219-236.
29. McCartney, H. A., Lacey, M. E., and Rawlinson, C. J. 1986. Dispersal of *Pyrenopeziza brassicae* from an oil-seed rape crop. J. Agric. Sci. 107:299-305.
30. Minogue, K. P. 1986. Disease gradients and the spread of disease. Pages 285-310 in: Plant Disease Epidemiology. K. J. Leonard and W. E. Fry, eds. MacMillan Publishing Co., Inc., New York.
31. Minogue, K. P., and Fry, W. E. 1983. Models for the spread of disease: Model description. Phytopathology 73:1168-1173.
32. Minogue, K. P., and Fry, W. E. 1983. Models for the spread of plant disease: Some experimental results. Phytopathology 73:1173-1176.
33. Mollison, D. 1977. Spatial contact models for ecological and epidemic spread. J. R. Statist. Soc. B 39:283-326.
34. Mundt, C. C., and Leonard, K. J. 1985. A modification of Gregory's model for describing plant disease gradients. Phytopathology 75:930-935.
35. Newhall, A. G. 1938. The spread of onion mildew by wind-borne conidia of *Peronospora destructor*. Phytopathology 28:257-269.
36. Pielou, E. C. 1975. Ecological Diversity. Wiley-Interscience, New York.
37. Raynor, G. S., Ogden, E. C., and Hayes, J. V. 1972. Dispersion and deposition of corn pollen from experimental sources. Agron. J. 64:420-427.
38. Roelfs, A. P. 1972. Gradients in horizontal dispersal of cereal rust uredospores. Phytopathology 62:70-76.
39. Schneiderhahn, F. J. 1926. Apple diseases in northern Virginia. Virginia Agric. Exp. Stn. Bull. 245:10-15.
40. Sokal, R. R., and Rohlf, F. J. 1981. Biometry. 2nd ed. W. H. Freeman & Co., San Francisco.
41. Sreeramulu, T., and Ramalingam, A. 1961. Experiments on the dispersion of *Lycopodium* and *Podaxis* spores in the air. Ann. Appl. Biol. 49:659-670.
42. Thieme, H. R. 1977. A model for the spatial spread of an epidemic. J. Math. Biol. 4:337-351.
43. van den Bosch, F., Frinking, H. D., Metz, J. A. J., and Zadoks, J. C. 1988. Focus expansion in plant disease. III: Two experimental examples. Phytopathology 78:919-925.
44. van den Bosch, F., Zadoks, J. C., and Metz, J. A. J. 1988. Focus expansion in plant disease. I: The constant rate of focus expansion. Phytopathology 78:54-58.
45. van den Bosch, F., Zadoks, J. C., and Metz, J. A. J. 1988. Focus expansion in plant disease. II: Realistic parameter-sparse models. Phytopathology 78:59-64.